Simple Functionalization Strategies for Enhancing Nanoparticle Separation and Recovery with Asymmetric Flow Field Flow Fractionation

ARTICLE *in* ANALYTICAL CHEMISTRY · JANUARY 2015

Impact Factor: 5.64 · DOI: 10.1021/ac503683n · Source: PubMed

5 AUTHORS, INCLUDING:

Thilak Mudalige
U.S. Food and Drug Administration
29 PUBLICATIONS **389** CITATIONS

SEE PROFILE

Haiou Qu
U.S. Food and Drug Administration
17 PUBLICATIONS **289** CITATIONS

SEE PROFILE

analytical chemistry

Article

pubs.acs.org/ac

Simple Functionalization Strategies for Enhancing Nanoparticle Separation and Recovery with Asymmetric Flow Field Flow Fractionation

Thilak K. Mudalige,* Haiou Qu, Germarie Sánchez-Pomales, Patrick N. Sisco, and Sean W. Linder*

Office of Regulatory Affairs, Arkansas Regional Laboratory, U.S. Food and Drug Administration, 3900 NCTR Road, Jefferson, Arkansas 72079, United States

Supporting Information

ABSTRACT: Due to the increasing use of engineered nanomaterials in consumer products, regulatory agencies and other research organizations have determined that the development of robust, reliable, and accurate methodologies to characterize nanoparticles in complex matrices is a top priority. Of particular interest are methods that can separate and determine the size of nanomaterials in samples that contain polydisperse and/or multimodal nanoparticle populations. Asymmetric-flow field flow fractionation (AF4) has shown promise for the separation of nanoparticles with wide size range distributions; however, low analyte recoveries and decreased membrane lifetimes, due to membrane fouling, have limited its application. Herein, we report straightforward strategies to minimize membrane fouling and improve nanoparticle recovery by functionalizing the surface of the nanoparticles, as well as that of the AF4 membranes. Gold nanoparticles (AuNP) were stabilized through functionalization with a phosphine molecule, whereas the surface of the membranes was coated with a negatively charged polystyrenesulfonate polymer. Improved nanoparticle separation, recoveries of 99.1 (±0.5) %, and a detection limit of 6 μg/kg were demonstrated by analyzing AuNP reference materials of different sizes (e.g., 10, 30, and 60 nm), obtained from the National Institute of Standards and Technology (NIST). Furthermore, the stability of the polymer coating and its specificity toward minimizing membrane fouling were demonstrated.

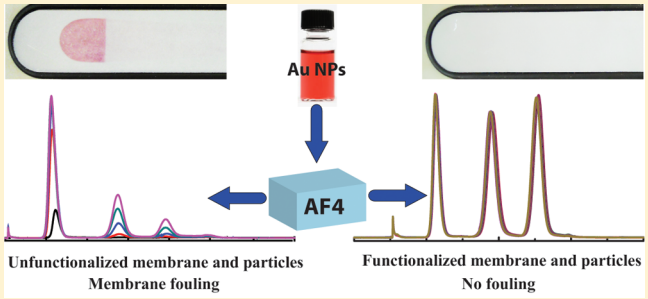

Metallic nanoparticles, such as gold, silver, and palladium, are utilized in many applications, including sensors, solar cells, foods, drugs, and other consumer products.[1−4] The physical and chemical properties of these nanoparticles are dependent on particle size; thus, the development of methodologies that can reliably and accurately determine mean particle size and size distribution is warranted.[5,6] Furthermore, size-based separation techniques are preferred for those samples consisting of nanoparticles with a wide size distribution or multimodal populations.[7,8] Unlike nanoscale biomolecules and polymeric particles which exhibit well-defined structures and high stability in solution phase, inorganic nanoparticles are not stable under the typical conditions used for separation, thus making their analysis a challenge.[9] Multiple techniques for the size-based separation of nanoparticles have been reported in the literature, including asymmetric-flow field flow fractionation (AF4), cyclic electrical field flow fractionation, size exclusion chromatography, capillary electrophoresis, centrifugation, and diafiltration.[9−13] Many publications highlight the utility and novelty of AF4 for the separation of nanomaterials.[14−21] Some advantages of AF4 over other size-based separation techniques include the following: (1) wide application range—it is capable of separating materials with high resolution over a wide size range, from the low nanometer size range up to micron size; (2) minimal sample preparation; and (3) its ability to interface with other instruments, such as dynamic light scattering (DLS) and inductively coupled plasma mass spectroscopy (ICP-MS).[15,22−26] AF4 has been applied for the size- and shape-based separation of nanoparticles such as gold, silver, and titanium dioxide in various conditions and used in tandem with detectors such as DLS and ICP-MS for size and elemental composition determination, respectively.[7,15,27,28]

In contrast to other separation techniques, AF4 does not utilize a stationary and mobile phase to separate analytes, but rather, the technique uses a narrow bore channel in which one side of the channel is composed of a porous membrane supported by a metallic frit. The AF4 channel assembly is schematically illustrated in Figure 1, and the basics of the separation process have been well explained in recent literature.[14,29−31] Sample analysis consists of two main steps: an initial focusing step, followed by a separation step. In the focusing step, as indicated in Figure 1b, sample is injected through the injection port, at the same time as both channel-in and channel-out ports pump liquid into the channel. The liquid

Received: October 1, 2014
Accepted: January 4, 2015
Published: January 4, 2015

DOI: 10.1021/ac503683n
Anal. Chem. 2015, 87, 1764−1772

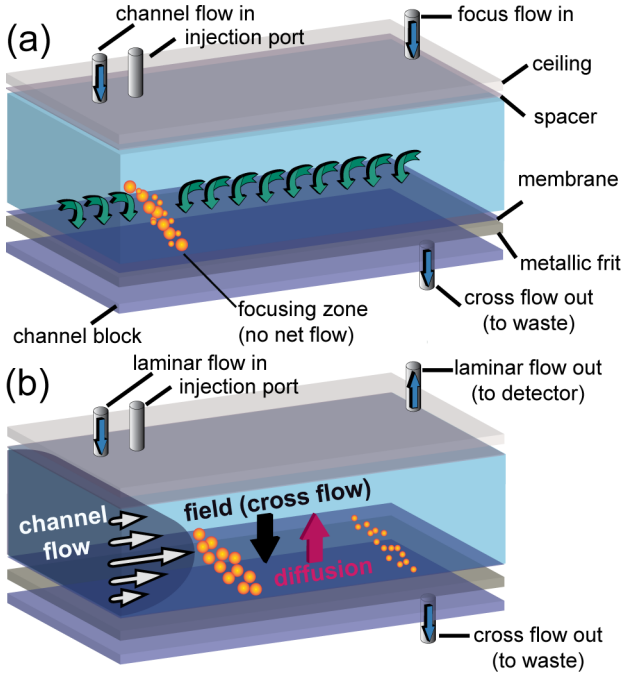

Figure 1. Schematic illustration of AF4 channel assembly showing the liquid flow profile during the (a) focusing and (b) separation steps.

escapes by passing through the porous membrane which creates a focusing zone, resulting in no net liquid flow along the channel. Any particulate matter within the sample becomes concentrated in the focusing zone and achieves an equilibrium distance from the membrane depending on the diffusion rate of the particles.[31] The sample focusing step is essential for minimizing peak broadening during sample injection and generating narrow peaks.[32]

Even though AF4 provides excellent separation, low nanoparticle recoveries and a decreased membrane lifetime due to the accumulation of solid particles on the membrane surface, also known as membrane fouling, have limited the potential use of this technology.[33] Accumulation of particles leading to membrane fouling at the focusing site of the channel is caused by the irreversible binding of the nanoparticles to the membrane.[34,35] Membrane fouling can be easily visualized when analyzing colored analytes, such as gold nanoparticles (AuNPs).[14,29] During the first few separation cycles after the application of a new membrane, AuNPs bind to the membrane surface, leading to poor nanoparticle recoveries. Recovery percentages gradually increase thereafter due to membrane saturation.[28] Herein, we report a novel methodology to improve the separation efficiency and recovery values of AuNPs through a process of stabilizing both the particles and the membranes. The particle−membrane interactions were altered by modifying AuNPs with phosphine, which adsorbs onto the AuNPs surface by chemisorption, and by coating the membrane surface with polystyrenesulfonate, an anionic water-soluble polymer.[5]

EXPERIMENTAL SECTION

Materials and Reagents. Type I ultrapure water (18 MΩ·cm), obtained from a Thermo Scientific Barnstead Nanopure System (Waltham, MA) was utilized for all solution preparations. Nitric acid (67%−69%), hydrochloric acid (34%−37%) (Optima grade), and sodium dodecyl sulfate (reagent grade) were purchased from Fisher Scientific (Houston, TX) and used for microwave-assisted digestion of samples and ICP-MS analysis. Gold (1000 ppm) single-element ICP-MS standard solutions were acquired from Spex CertiPrep (Metuchen, NJ) and Ultra Scientific (Kingstown, Rhode Island). Bismuth (100 ppm) single-element ICP-MS standard solution was purchased from Inorganic Ventures (Christiansburg, VA). Sodium chloride (ACS reagent grade), isopropanol (HPLC grade), bis(*p*-sulfonatophenyl)phenylphosphine (phosphine), polyethylene glycol (PEG; average molecular weight: 100 kDa), poly(sodium 4-styrenesulfonate) (average molecular weight: 70 kDa) were purchased from Sigma-Aldrich (Saint Louis, MO). Fluorescein-labeled polystyrenesulfonate, with a monomer to fluorophore ratio of 112:1, was acquired from Surflay Nanotech GmbH (Berlin, Germany). AuNPs reference materials—with nominal diameters of 10 (RM8010), 30 (RM8012), and 60 (RM8013) nm—were purchased from the National Institute of Standards and Technology (NIST, Gaithersburg, MD). Both 5 and 30 nm tannic acid stabilized gold nanoparticles were obtained from NanoComposix, Inc. (San Diego, CA). NADIR precut regenerated cellulose membranes with a molecular weight cutoff of 5 kDa (5 kDaNC), Millipore precut regenerated cellulose membrane with a molecular weight cutoff of 30 kDa (30 kDaMC), and polyethylene sulfone (PES) membranes with a molecular weight cutoff of 10 kDa (10 kDaPES) were purchased from Wyatt Technology (Santa Barbara, CA). Carbon-coated copper grids (300 mesh), from Electron Microscopy Sciences (Hatfield, PA), were used to prepare samples for the analysis by transmission electron microscopy (TEM). Amicon Ultra 0.5 mL centrifugal filter units with a molecular weight cutoff of 3 kDa were purchased from EMD Millipore (Billerica, MA) and used to remove excess phosphine. Solvent-resistant disposable microcuvettes, disposable folded capillary cells, and surface zeta potential accessory, from Malvern Instruments (Worcestershire, UK), were used for particle sizing, measuring particle zeta potential, and measuring membrane surface zeta potential, respectively.

Functionalization and Characterization Methods. *Gold Nanoparticle Functionalization.* Phosphine-coated AuNPs suspensions were prepared by mixing citrate-stabilized AuNPs reference materials with the required amount of phosphine to keep the phosphine concentration constant, at 0.5 mg/mL. After the phosphine was added, the solutions were vortexed at room temperature for 2 min to assist with the exchange of citrate molecules with phosphine. Phosphine-coated AuNPs were used directly for AF4 analysis. For size and zeta potential measurements, the functionalized particles were isolated by centrifugation, using 3 kDa molecular weight cutoff centrifugal filter units, and subsequently suspended in the appropriate solvent.

Determination of Particle Size and Zeta Potential. Particle size and zeta potential measurements were performed using a Malvern Instruments (Worcestershire, U.K.) Zetasizer Nano ZS DLS system. For particle size determination, approximately 50 μL of each sample was added to low-volume disposable cuvettes and allowed to equilibrate at 25 °C for 120 s prior to analysis. All particle sizes reported here were obtained from intensity-based distributions and represent the average and standard deviation of three measurements. Samples for zeta potential measurements were prepared by diluting the AuNPs solutions with 1 mM NaCl to match the ionic strength and composition of the AF4 carrier fluid. Measurements were

DOI: 10.1021/ac503683n
Anal. Chem. 2015, 87, 1764−1772

performed using a disposable folded capillary cell from Malvern.

AuNPs standards were studied on a JEOL 1400 TEM (Peabody, MA, U.S.A.) operated at 80 kV. A few drops of sample were placed directly on a 300 mesh copper grid and air-dried overnight. The micrographs were acquired by a TVIPS TemCam F416 camera, and ImageJ software was used in the processing of images to obtain size statistics of AuNPs. Five hundred particles were measured for the accurate statistics.

Determination of Particle Concentration and Recovery by ICP-MS. Quantification of gold in nanoparticle standards and recovered particles from AF4 was carried out by ICP-MS. Briefly, a calculated volume of nanoparticle suspension was added to microwave digestion vessels and digested for 30 min with 2 mL of nitric acid and 1 mL of hydrochloric acid using a CEM (Matthews, NC) MARS 5 microwave accelerated reaction system (CEM MARSXpress Teflon vessels; CEM MARSXpress vessel capping station). The samples were subsequently analyzed by an Agilent Technologies (Santa Clara, CA) 7700x ICP-MS (Micro mist nebulizer; autosampler ASX-500; MassHunter workstation software version A.01.02) under no collision cell gas mode (standard mode). A 6-point calibration curve with bismuth as an internal standard and a second source gold ICP-MS standard for independent calibration verification was used for analysis.

Nanoparticle Separation and Analysis by AF4. A Wyatt Technology (Santa Barbara, CA) short channel Eclipse 3 AF4 system composed of a flow control unit and channel compartment (short channel with 145 mm length and 350 μm spacer) was coupled to an Agilent Technologies (Santa Clara, CA) 1200 high-performance liquid chromatography (HPLC) system, which contains a pump (G1310A), auto sampler (G1329B) and UV−vis detector (G1315D). GASTORR AG series TG-14 multichannel degasser was used to degas the carrier fluid prior to analysis. A PVDF hydrophilic 0.1 μm membrane filter (EMD Millipore, Billerica, MA) was used just after the pump. The pump was used to control liquid flow into the channel compartment and an auto sampler was used for sample introduction.

Precut membranes were soaked overnight in 20% isopropanol, washed with Type I ultrapure water, and equilibrated with carrier fluid inside the AF4 channel for 1 h. AuNPs sample was prepared by mixing equal volume of 50 mg/L solution of 10, 30, and 60 nm NIST standards, resulting in a final concentration of 16.7 mg/L for each size of the particles. An identical procedure was followed for tannic-acid-coated 5 and 30 nm particles with an achieved final concentration of 25 mg/L for the each size component. 100 μL of sample was analyzed during each run using the conditions listed in Table 1. The absorbance signal was collected at a wavelength of 520 nm using a 10 nm bandwidth with respect to the 890 nm reference peak. To determine the nanoparticle recovery, 100 μL of AuNP suspension was injected to the system, and eluates were collected to a 100.0 mL grade A volumetric flask. Recovery values were calculated with respect to same amount of nanoparticles passed through the system without cross-flow, as previously described.[28]

Table 1. Liquid Flow Program for Nanoparticle Analysis

step	designation	time (min), channel & cross flow (mL/min)
1	elution (pre focus)	0.00−1.0, CF 1.0 cross flow 0.0
2	focus	1.0−2.0, CF 1.0 cross flow 1.5
3	focus + injection	2.0−4.0, CF 1.0 cross flow 1.5, injection flow 0.2
4	focus	4.0−5.0, CF 1.0 cross flow 1.5
5	gradient elution	5.0−30.0, CF 1.0 cross flow 2.0 to 0.0
6	elution	30.0−40.0, CF 1.0 cross flow 0.0

Analysis of the Membranes by Scanning Electron Microscopy (SEM). Membranes were carefully removed from the AF4 channel, cut to the appropriate size with a pair of scissors, and dried in a vacuum desiccator for 12 h. The dried membranes were mounted on aluminum SEM stubs using conductive carbon tape and carbon coated in an Edwards Auto 306 thermal evaporator (Edwards Limited, Sanborn, NY) to minimize sample charging during SEM analysis. SEM images were collected with a Zeiss Merlin field emission scanning electron microscope (Jena, Germany) using an in-lens energy-selective backscattered detector at a 2 mm working distance and a 5 kV acceleration voltage. Energy dispersive X-ray fluorescence spectra were collected at 20 kV acceleration voltages and a 10.2 mm working distance using an EDAX (Mahwah, NJ) Apollo XL detector.

RESULTS AND DISCUSSION

The theoretical background of AF4 has been described thoroughly in the literature.[29] In AF4, the determination of the retention ratio (R), which is the ratio between retention time (t_r) and dead time (t_0), is described by eq 1, where V_0 denotes channel void volume, V_c denotes cross-flow rate, w is channel thickness, and D is the analyte diffusion coefficient.[36] This equation accounts for particle diffusion and cross-flow-to-channel flow ratio for any given channel dimension; however, it neglects to take under consideration the profound effect which membrane−particle interactions can have on retention time. Numerous forms of interactions between the membrane and the particles such as electrostatic, ionic, and hydrophobic, can occur.[34,37] The types of interactions and their associated strength depend on the membrane material composition, particle coating, elemental composition of particles, and electrolytes in the mobile phase; therefore, all of these factors need to be considered in the development of improved methodologies for the separation of particles using AF4.[38] In this study, we focused on minimizing membrane fouling and increasing nanoparticle recovery rates by changing the composition of the carrier fluid, the membrane type, membrane coating, and particle coating, while keeping liquid flow parameters constant, as indicated in Table 1.[28]

$$R = \frac{t_0}{t_r}, \quad t_r = \frac{t_0 V_c w^2}{6 D V_0} \tag{1}$$

To evaluate the need for the presence of an electrolyte in the carrier fluid, mixtures of citrate-coated 10, 30, and 60 nm AuNPs were analyzed using water and 1 mM sodium chloride solution as the carrier fluid, and 5 kDaNC, 30 kDaMC, and 10 kDaPES membranes.[39] In the case of water as the carrier fluid, peak separation was not satisfactory, as evidenced by the very short retention times for the particles, and by the large void peak present in the fractogram of each of the studied membranes. Four consecutive fractograms using 5 kDaNC membranes are shown in Figure 2a. Similar results were obtained using various types of membranes (30 kDaMC and 10 kDaPES, data not shown). We also observe accumulation of particles on membranes primarily at the focusing zone.

DOI: 10.1021/ac503683n
Anal. Chem. 2015, 87, 1764−1772

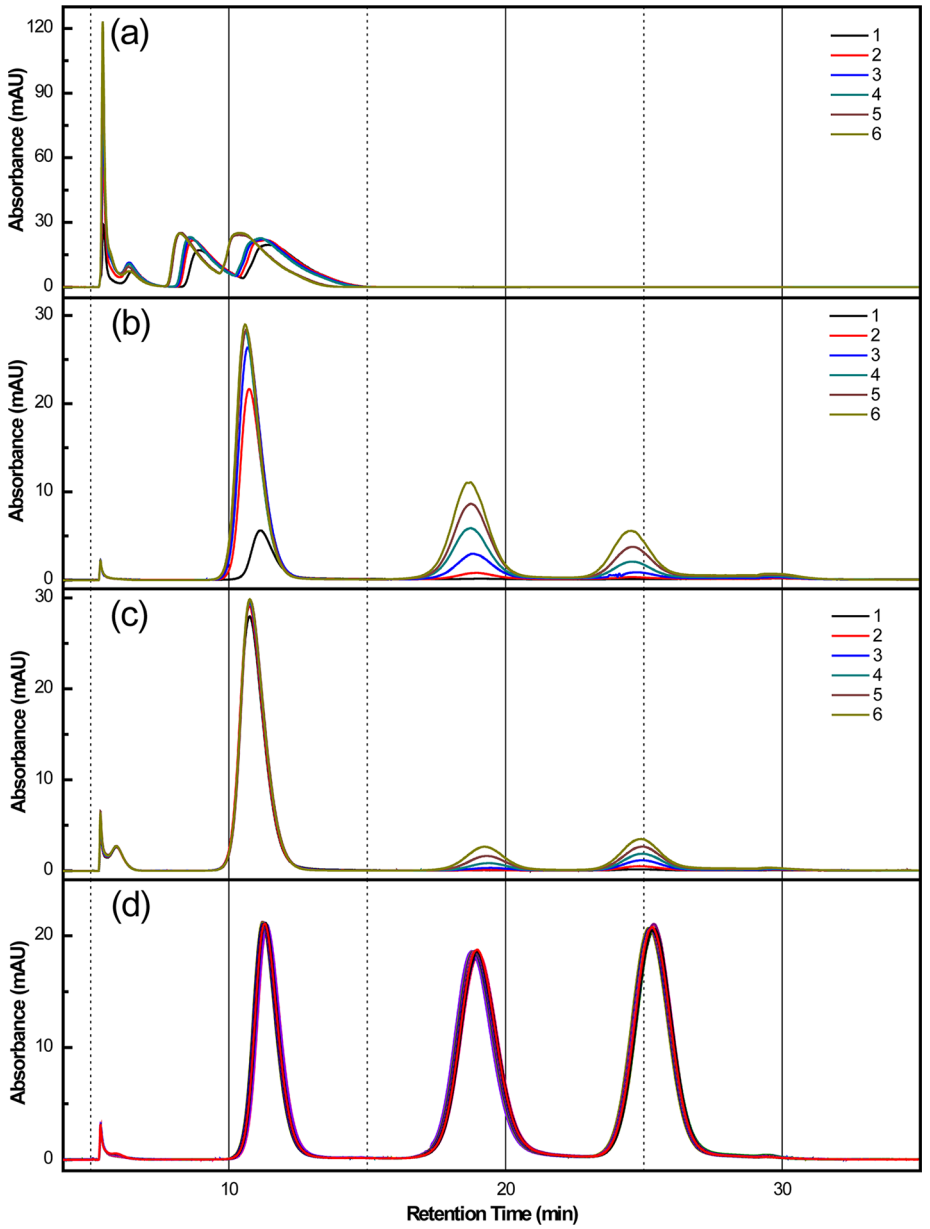

Figure 2. AF4 fractograms of (a) citrate-coated AuNPs, using water as carrier fluid, and a 5KDaNC membrane (b) citrate-coated AuNPs, using 1 mM NaCl as carrier fluid, and a 5KDaNC membrane (c) phosphine-coated AuNPs, using 1 mM NaCl as carrier fluid, and a polyethylene glycol-coated 5KDaNC membrane, and (d) 30 consecutive injections of phosphine-coated AuNPs, using 1 mM NaCl as carrier fluid, and a PSS-coated 5KDaNC membrane.

It is well documented that the presence of electrolyte in the carrier fluid is necessary because the electrostatic repulsion between the particles and membrane is reduced allowing particles to equilibrate closer to the membrane and results in longer retention of the analyte and subsequent separation in AF4.[40] The application of 1 mM NaCl as a carrier fluid results in better baseline separation with longer retention times, but particle recovery is sacrificed. Also, patches of accumulated particles were clearly visible on the membrane. Particle recovery was not satisfactory for 5 kDaNC (Figure 2b), and identical results were observed for 30 kDaMC and 10 kDaPES membranes (Supporting Information, Figure S1). Using identical conditions (citrate-coated AuNPs and 1 mM NaCl), low recovery was observed in previous publications.[28] Electrolytes other than NaCl can be probed to potentially increase separation, including acids and bases to change the pH of the carrier fluid; however, citrate-coated particles are known to aggregate with a slight reduction of pH.[41] Membrane fouling was found to be size dependent; for example, 60 nm particles exhibited the lowest recovery compared to 30 and 10 nm AuNPs. The amount of particles recovered increased with decreasing particle size. The higher degree of particle loss for the 60 nm particles can be rationalized due to the equilibration distance of the particles during the analysis process. Although equilibrating the particles closer to the membrane during analysis provides longer retention and enhanced separation, it also promotes membrane fouling.[40] In consecutive fractograms, a run-to-run increase in recovery was observed. The first few cycles exhibited lower recoveries, resulting in an inability of the membrane to retain further particles, as previously reported by other researchers on multiple occasions.[42] In the AF4 analysis process, the sample is injected into a large volume of carrier

DOI: 10.1021/ac503683n
Anal. Chem. 2015, 87, 1764−1772

fluid leading to a loss of the protective coating on the particles, exposing the particles to a high ionic strength environment, which shields the electrostatic repulsion between particles. Furthermore, membrane fouling is prominent at the focusing zone, where particles are concentrated to a small zone near the injection port.[42] This zone is an area of no net liquid flow along the channel and essentially zero shear force along the membrane from the carrier fluid in the focusing.

For consistent recovery throughout consecutive runs, membrane fouling has to be minimized; therefore, we introduced a stable particle coating and membrane functionalization to alter particle−membrane interactions. In general, metallic nanoparticle solutions are colloidal suspensions stabilized by their charge and interparticle electrostatic repulsion.[5] Typically, metallic nanoparticles are charge-stabilized by the adsorption of small, highly charged, organic molecules such as citrate, tannic acid, cetyltrimethylammonium bromide, malate, or sodium dodecyl sulfate.[5] In some cases, long chain polymers such as starch, polyvinyl pyrimidine, polystyrene sulfate, and polyacrylic acids are used as stabilizers. These polymers act as a physical barrier which prevents aggregation, as well as giving the nanoparticles a surface charge.[5] In most cases, these nanoparticle stabilizers are physisorbed to the metallic surface by weak electrostatic bonding and are in equilibrium with free stabilizers floating in the surrounding media.[43]

Here we replace the citrate on the AuNPs surface with a more stable, negatively charged, phosphine coating (bis(*p*-sulfonatophenyl)phenylphosphine). The phosphine molecules are bound to the nanoparticle surface by chemisorption, which is a stronger bond type when compared to the physisorption of citrate.[44,45] In comparison to citrate-coated particles, phosphine-coated particles are stable in high ionic strength conditions. Due to the weak interactions between citrate and the nanoparticle surface, the former can be washed off during the focus injection and focusing steps, leading to destabilization of the particles, membrane fouling, and particle aggregation. We continued method development using phosphine-coated particles as a strategy to stabilize the particles and increase AF4 nanoparticle recovery due to their stability.[46]

Citrate-coated NIST AuNPs standards, with nominal sizes of 10, 30, and 60 nm, were functionalized with phosphine.[47] To evaluate the effect of functionalization on the properties of the particles, average particle size and zeta potential values were measured prior to and after phosphine functionalization. The hydrodynamic diameter values obtained for the citrate-coated and phosphine-coated AuNPs were in good agreement with the nominal particle size reported by NIST (Supporting Information, Table S1). Representative TEM images are available in the Supporting Information (Figures S3−S5). Zeta potential measurements of the 30 and 60 nm AuNPs revealed no discernible changes in zeta potential values upon functionalization with phosphine (Supporting Information, Table S1). Furthermore, the formation of a stable phosphine coating on nanoparticles was verified by observation of particle stability in 100 mM NaCl solution.[47] Zeta potential values for 5 and 10 nm AuNPs were not reported because accurate determination of zeta potential values for small nanoparticles utilizing the instrumentation and settings used in these studies is quite challenging.

To evaluate the electrostatic interactions between nanoparticles and the AF4 membrane, we determined the zeta potential value of the nonfunctionalized membrane surface. This measurement was performed using a surface zeta potential cell accessory along with tracer particles, by measuring the particles mobility at varying distances from the membrane surface. A detailed description of the materials and methods used for this type of measurements is available as Supporting Information. The calculated surface zeta potential values were −32.9 (±1.8) mV for the 5 kDaNC membrane, −28.2 (±2.3) mV for the 30 kDaMC membrane, and −34.3 (±1.9) mV for the 10 kDaPES membrane.

Zeta potential values for the membranes and the particles have been used as a key parameter in the study of membrane fouling, because particle and membrane surface chemistry, particle−membrane interactions, as well as the ionic environment, have an effect on membrane fouling. In essence, zeta potential measures the magnitude of the electrostatic interactions between charged surfaces (e.g., nanoparticles and membranes in an electrolyte solution); it can therefore provide some insight on the stability of colloidal dispersions and on membrane fouling. For example, fouling is minimal when membranes with high negative zeta potential values come in contact with negatively charged particles due to the electrostatic repulsion between species of same charge. Negative surface charge on membranes can be attributed to the ionization of functional groups on the membrane surface and/or the adsorption of negatively charged ions on the surface of membranes, which is a common phenomenon for hydrophobic surfaces such as PES.[48,49] Zeta potential itself cannot completely explain membrane fouling in this case. Consideration must also be given to other interactions such as van der Waals, hydrophobic, and dipole−dipole interactions, which all play prominent roles in particle−membrane interactions.

In addition to nanoparticle surface modification, another effective strategy to improve recovery is to functionalize the AF4 membrane with a charged polymer. The application of a polymer coating can also be an effective route to minimize membrane fouling by altering the membrane to particle interactions. Because the lowest nanoparticle recovery was observed using 5 kDaNC membranes, 1 mM NaCl carrier fluid, and citrate-coated particles, these conditions were selected for additional method development. We selected polystyrenesulfonate, a negatively charged polymer with sufonate functional groups, to modify the AF4 membrane coating. We injected the polymer solution using the same methodology as a sample injection; however, no gradient elution step was performed. The membrane was coated using three 100 μL injections of polymer at a concentration of 5 mg/mL. The coating step was followed by 30 consecutive injections of phosphine-coated nanoparticles resulting in no particle accumulation on the membrane or run-to-run variation between chromatograms (Figure 2d). This indicates the stability of the polymer coating on the membranes and minimization of membrane fouling. For further verification, nanoparticle recovery was measured by ICP-MS analysis of the eluent from three 100 μL injections of a 30 nm NIST standard nanoparticle solutions with focusing and cross-flow using same separation methodology, and without focusing and cross-flow for comparison as previously published.[16,28] Calculated recoveries for 30 nm particles are 99.1 (±0.5) % for three runs. The detection limit of the methodology was calculated by the 3 sigma (3σ) method and found to be 6 μg/kg for each size fraction using ICP-MS as a detection platform. The applicability of the developed methodology for particles stabilized with entities other than citrate was assessed using tannic-acid-stabilized 5 and 30 nm AuNPs.

DOI: 10.1021/ac503683n
Anal. Chem. 2015, 87, 1764−1772

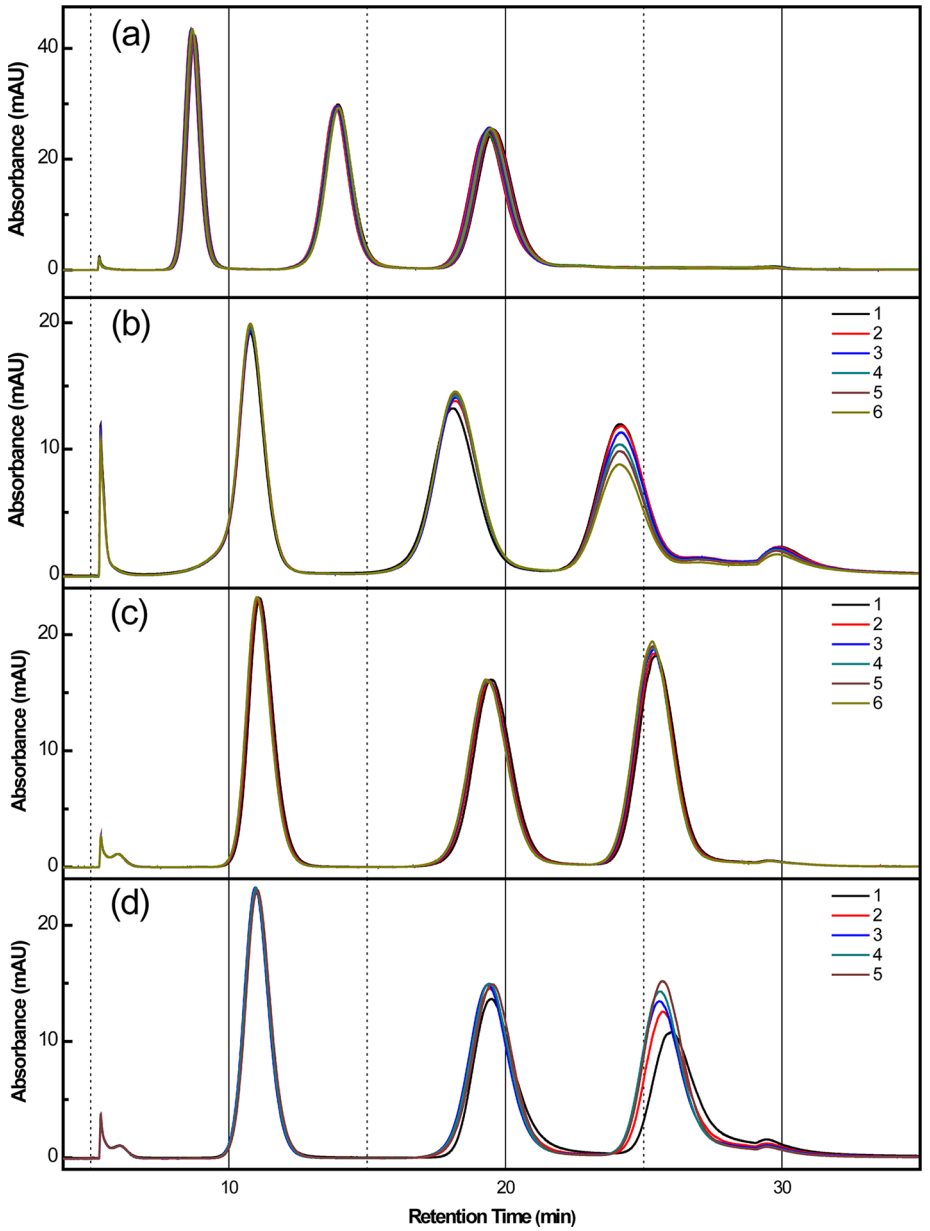

Figure 3. AF4 fractograms of (a) 20 consecutive injections of phosphine-coated AuNPs, using 1 mM NaCl as carrier fluid, and a PSS-coated 30 kDaMC membrane (20 consecutive injections); (b) phosphine-coated AuNPs, using 1 mM NaCl as carrier fluid, and a PSS-coated 10 kDaPES membrane; (c) phosphine-coated AuNPs, using 2 mM NaCl as carrier fluid, and a PSS-coated 5 kDaNC membrane; and (d) phosphine-coated AuNPs, using 5 mM NaCl as carrier fluid, and a PSS-coated 5 kDaNC membrane.

Tannic acid is a polyphenolic compound, and its structure is available in Figure S12 of the Supporting Information. It was found that the ligand exchange of tannic acid with phosphine coating provided consistent results without membrane fouling and run to run variation. Tannic acid coated gold nanoparticles showed longer retention times compared to phosphine coted particles (Supporting Information, Figure S2). This observation can be attributed to the less negative zeta potential of the tannic-acid-coated particles, which allows the particles to equilibrate much closer to the membrane resulting in longer retention times. Furthermore, recovery for tannic-acid-stabilized particles was about 20% lower than phosphine-coated particles in the both 5 and 30 nm particles. The particles lost due to membrane fouling may be the reason for the lower recovery of tannic-acid-coated particles. For verification of recovery, the absorbance spectra of tannic-acid-stabilized particles and those treated with phosphine were measured, and no significant difference was observed. Further additional studies on application of developed methodology for particle having different composition and coating are underway.

To evaluate the polymer specificity for the prevention of membrane fouling, polyethylene sufonate was replaced with polyethylene glycol at an identical concentration. Six consecutive fractograms were collected using 1 mM NaCl as a carrier fluid. This analysis resulted in membrane fouling with low particle recovery (Figure 2c); particles were clearly visible on the membrane at the focusing zone (Figure 4b). According to these findings, the prevention of membrane fouling is polymer specific, and the smoothing (reducing membrane roughness) of the membrane surface by polymer coating might not be a factor.[50] Furthermore, we evaluated citrate-coated particles with a PSS-coated membrane and phosphine-coated

DOI: 10.1021/ac503683n
Anal. Chem. 2015, 87, 1764−1772

particles with an uncoated membrane using 1 mM NaCl as the carrier fluid. In both cases, the recovery was not maximized, indicating that the mutual benefit of a coated membrane and a coated nanoparticle is needed to make the most impact on recovery.

Furthermore, polymer-coated 30 kDa Millipore regenerated cellulose (30 kDaMC) membranes and polymer-coated 10 kDa polyethylene sulfone (10 kDaPES) membranes were evaluated with phosphine-coated particles using 1 mM NaCl as carrier fluid. The results for the 30 kDaMC polymer-coated membranes were identical to 5 kDa NADIR regenerated cellulose membranes (5 kDaNC) membrane with excellent recovery for 20 consecutive injections (Figure 3a); however, in the case of the 10 kDaPES coated membrane, there was continuous loss in the recovery, which may indicate an increase in membrane fouling and the possibility of polymer instability on the membrane (Figure 3b). Even though 1 mM sodium chloride is sufficient for nanoparticle separation, we evaluated the feasibility of a methodology using an elevated sodium chloride concentration and 5 kDaNC. We did not observe any membrane fouling or particle loss using 2 mM NaCl as a carrier fluid (Figure 3c), but in the case of 5 mM NaCl as running media, we observed both particle loss and run-to-run increase in signal (Figure 3d).

We further evaluated the stability of polystyrene sufonate (PSS) on 5 kDaNC membranes using 1 mM SDS as the carrier fluid. SDS is a well utilized detergent in AF4, which can destabilize the polymer on the membrane surface. We collected 10 consecutive fractograms (Supporting Information, Figure S1a), which did not indicate any membrane fouling or particle loss. In the case of the SDS carrier fluid, the retention times for all three sizes of particles decreased when compared to identical concentrations of sodium chloride, indicating the reduction of membrane−particle interactions. We further washed the membrane with 500 mL of 1 mM SDS at a channel flow rate of 1 mL/min and collected another set of fractograms (Supporting Information, Figure S1b). This second set of fractograms indicated an increase in run-to-run loss of particles, which may be a result of continuous loss of the polymer coating with prolonged washing.

To confirm stable polymer layer formation, we used fluorescently tagged polystyrenesulfonate to visualize the polymer coating via florescent imaging, and we found a clear patch of fluorescent signal even after 30 consecutive runs. This indicates the stability of the polymer coating on the membrane (Supporting Information, Figure S11). The focusing area of the membranes was also examined with SEM for visualization of nanoparticle attachment. Nanoparticles were found on 5 kDaNC membranes after six consecutive runs with citrate-coated particles using 1 mM NaCl as carrier fluid, and on PEG-coated 5 kDaNC cellulose membrane after six consecutive runs of phosphine-coated particles with 1 mM NaCl. Representative SEM images can be seen in Figure 4a,b with an inset of the optical image of the focusing zone. Even though the extent of particle loss is somewhat equivalent in both cases, according to the fractograms, visual images indicate a more intense reddish color in the PEG-coated membranes with phosphine-coated particles. This is an indication of particle aggregation in the first case where citrate-coated particles are used. The reddish color of AuNPs diminishes upon aggregation due to an absorbance shift to higher wavelengths caused by the coupling of surface plasmon between nanoparticles.[51] Aggregates of particles are visible in SEM images, indicating the instability of citrate-coated

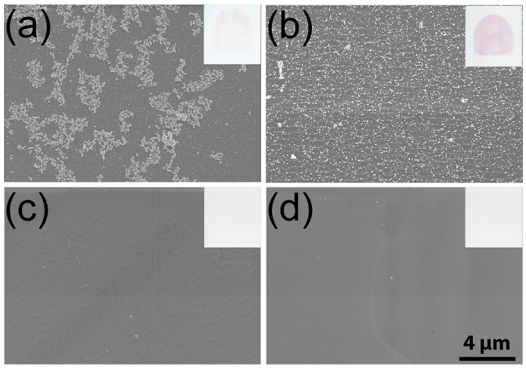

Figure 4. Scanning electron micrographs and digital images (inset) of the focusing zone of the membrane for the following: (a) a 5 kDaNC membrane after six consecutive injections of citrate-coated AuNPs, using 1 mM NaCl as running media; (b) a polyethylene glycol-coated 5 kDaNC membrane after six consecutive injections of phosphine-coated AuNPs, using 1 mM NaCl as running media; (c) a PSS-coated 5 kDaNC membrane after 30 consecutive injections of phosphine-coated AuNPs, using 1 mM NaCl as running media; and (d) an uncoated 5 kDaNC membrane equilibrated overnight in running media.

particles under these conditions. We verified the identity of AuNPs seen by SEM by the collection of energy dispersive X-ray spectra (EDX) (Supporting Information, Figure S6a). EDX was also collected on bare AF4 membranes (Supporting Information, Figure S6b). Even after 30 consecutive runs with phosphine-coated particles, using 1 mM NaCl as the carrier fluid, no nanoparticles were found adhered to PSS-coated 5 kDaNC membranes. This indicates the prevention of membrane fouling, as illustrated in Figure 4c. SEM images of unused membranes are presented in Figure 4d for comparison.

Retention time and chromatographic resolution were calculated using the United States Pharmacopeia methodology (tangent method/Table 2). All the data shown here is averaged,

Table 2. Calculated Retention Times and Peak Resolution

	retention time (minutes)			resolution	
experimental conditions	10 nm	30 nm	60 nm	10 and 30	30 and 60
5 kDaNC 1 mM NaCl	6.34 (±0.02)	14.03 (±0.14)	20.42 (±0.11)	3.64 (±0.06)	2.51 (±0.01)
5 kDaNC 2 mM NaCl	6.03 (±0.04)	14.38 (±0.07)	20.36 (±0.04)	3.82 (±0.02)	2.29 (±0.01)
5 kDa NC 5 mM NaCl	5.98 (±0.03)	14.44 (±0.07)	20.71 (±0.17)	3.78 (±0.01)	2.27 (±0.02)
5 kDaNC 1 mM SDS	4.41 (±0.01)	10.43 (±0.03)	16.29 (±0.02)	3.57 (±0.02)	2.53 (±0.02)
30 kDaMC 1 mM NaCl	3.71 (±0.05)	9.05 (±0.11)	14.60 (±0.18)	3.73 (±0.01)	2.60 (±0.02)

and the standard deviation was calculated using five consecutive runs of phosphine-coated particles and PSS-coated membranes. As a result, 30 kDaMC membranes showed the best resolution throughout the size range of analysis. We observed no significant change in retention time for 5 kDaNC membranes with an increase in NaCl concentration(1, 2, and 5 mM), but in the case of 1 mM SDS as the carrier fluid, all three sizes of nanoparticles had shorter retention times, when compared to the identical ionic strength carrier fluid of 1 mM NaCl. Even though 30 kDaMC membranes using a 1 mM NaCl carrier fluid resulted in the shortest retention times for all the sizes of

DOI: 10.1021/ac503683n
Anal. Chem. 2015, 87, 1764−1772

nanoparticles, narrow peaks helped achieve identical resolution as in the case of 5 kDaNC membranes in similar running conditions. Peak widths for 5 kDaNC membranes are 1.63 (±0.01), 2.60 (±0.02) and 2.51 (±0.02) minutes in ascending order of particle size, which are larger than the corresponding widths for the 30 kDaMC membrane at 1.04 (±0.01), 1.82 (±0.01) and 2.44 (±0.01) min.

CONCLUSION

In summary, we have investigated the necessity of particle stabilization and membrane functionalization to improve nanoparticle recovery using AF4. We have developed a method that allows for the reliable separation of AuNPs with minimum particle loss and excellent recovery rate. Using this simple functionalization methodology, we were able to obtain AuNPs recovery values of 99.1 (±0.5) %.

Three membranes of differing composition were used in this study, all having identical zeta potential values under the same running conditions. Particle stabilization was achieved by self-assembly of a stable coating on the AuNPs surface. The coated particles can be used for AF4 analysis without further purification. We also developed a simple methodology to modify the AF4 membrane surface properties through adsorption of a negatively charged polymer (polystyrenesulfonate). The stability of the polymer coating was tested and confirmed under strong detergent conditions, such as SDS. We further confirmed the stability of the polymer coating on cellulose-based membranes using fluorescently tagged polystyrenesulfonate. The fluorescent signal could be seen even after 30 analyses, indicating polymer stability on the membrane surface. Polymer specificity for membrane fouling was demonstrated with the use of PEG. The PEG membrane coating was unable to improve particle recovery and led to particle loss greater than that corresponding to a regular membrane.

The application of AF4 for the reliable separation of nanoparticles has been limited due to low nanoparticle recovery rates and membrane fouling. Nevertheless, the outcome of this report opens the door for reliable separation methodologies for nanoparticles with stable coatings. Further studies on the effect of coating materials on recovery and the application of this developed methodology for the characterization of commercial products containing nanoparticles are underway.

ASSOCIATED CONTENT

Supporting Information

Additional information as noted in text. This material is available free of charge via the Internet at http://pubs.acs.org.

AUTHOR INFORMATION

Corresponding Authors

* (T.K.M) E-mail: Thilak.Mudalige@fda.hhs.gov. Phone +1-870-543-4665. Fax: +1-870-543-4041.

* (S.W.L.) E-mail: Sean.Linder@fda.hhs.gov. Phone: +1-870-543-4667. Fax: +1-870-543-4041.

Notes

The authors declare no competing financial interest.

ACKNOWLEDGMENTS

These studies were conducted using the Nanotechnology Core Facility (NanoCore) located on the U.S. Food and Drug Administration's Jefferson Laboratories campus (Jefferson, AR), which houses the FDA National Center for Toxicological Research and the FDA Office of Regulatory Affairs Arkansas Regional Laboratory. We thank Dr. Selen Stromgren, Dr. Anil Patri, Dr. Paul C. Howard, Dr. Jin-Hee Lim, and Dr. Ivan Quevedo for their support and valuable comments on the draft manuscript. This project was supported in part by an appointment to the Research Participation Program at the Office of Regulatory Affairs/Arkansas Regional Laboratory, U.S. Food and Drug Administration, administered by the Oak Ridge Institute for Science and Education through an interagency agreement between the U.S. Department of Energy and FDA. The views expressed in this document are those of the researchers and should not be interpreted as the official opinion or policy of the U.S. Food and Drug Administration, Department of Health and Human Services, or any other agency or component of the U.S. government. The mention of trades names, commercial products, or organizations is for clarification of the methods used and should not be interpreted as an endorsement of a product or manufacturer.

REFERENCES

(1) Alivisatos, P. *Nat. Biotechnol.* **2004**, *22*, 47−52.
(2) Bouwmeester, H.; Dekkers, S.; Noordam, M. Y.; Hagens, W. I.; Bulder, A. S.; de Heer, C.; ten Voorde, S. E. C. G.; Wijnhoven, S. W. P.; Marvin, H. J. P.; Sips, A. J. A. M. *Regul. Toxicol. Pharmacol.* **2009**, *53*, 52−62.
(3) Catchpole, K. R.; Polman, A. *Opt. Express* **2008**, *16*, 21793−21800.
(4) Hughes, G. A. *Nanomed. Nanotechnol.* **2005**, *1*, 22−30.
(5) Daniel, M. C.; Astruc, D. *Chem. Rev.* **2003**, *104*, 293−346.
(6) Kelly, K. L.; Coronado, E.; Zhao, L. L.; Schatz, G. C. *J. Phys. Chem. B* **2002**, *107*, 668−677.
(7) Hagendorfer, H.; Kaegi, R.; Parlinska, M.; Sinnet, B.; Ludwig, C.; Ulrich, A. *Anal. Chem.* **2012**, *84*, 2678−2685.
(8) Loeschner, K.; Navratilova, J.; Legros, S.; Wagner, S.; Grombe, R.; Snell, J.; von der Kammer, F.; Larsen, E. H. *J. Chromatogr. A* **2013**, *1272*, 116−125.
(9) Kowalczyk, B.; Lagzi, I.; Grzybowski, B. A. *Curr. Opin. Colloid Interface Sci.* **2011**, *16*, 135−148.
(10) Hinterwirth, H.; Wiedmer, S. K.; Moilanen, M.; Lehner, A.; Allmaier, G.; Waitz, T.; Lindner, W.; Lammerhofer, M. *J. Sep. Sci.* **2013**, *36*, 2952−2961.
(11) Franze, B.; Engelhard, C. *Anal. Chem.* **2014**, *86*, 5713−5720.
(12) Tasci, T. O.; Johnson, W. P.; Fernandez, D. P.; Manangon, E.; Gale, B. K. *Anal. Chem.* **2013**, *85*, 11225−11232.
(13) Sweeney, S. F.; Woehrle, G. H.; Hutchison, J. E. *J. Am. Chem. Soc.* **2006**, *128*, 3190−3197.
(14) Messaud, F. A.; Sanderson, R. D.; Runyon, J. R.; Otte, T.; Pasch, H.; Williams, S. K. R. *Prog. Polym. Sci.* **2009**, *34*, 351−368.
(15) Schmidt, B.; Loeschner, K.; Hadrup, N.; Mortensen, A.; Sloth, J. J.; Bender Koch, C.; Larsen, E. H. *Anal. Chem.* **2011**, *83*, 2461−2468.
(16) Dubascoux, S.; Von Der Kammer, F.; Le Hecho, I.; Gautier, M. P.; Lespes, G. *J. Chromatogr. A* **2008**, *1206*, 160−165.
(17) Giddings, J. C.; Caldwell, K. D. *Anal. Chem.* **1984**, *56*, 2093−2099.
(18) Zattoni, A.; Rambaldi, D. C.; Reschiglian, P.; Melucci, M.; Krol, S.; Garcia, A. M. C.; Sanz-Medel, A.; Roessner, D.; Johann, C. *J. Chromatogr. A* **2009**, *1216*, 9106−9112.
(19) Lohrke, J.; Briel, A.; Mäder, K. *Nanomedicine* **2008**, *3*, 437−452.
(20) Collins, M. E.; Soto-Cantu, E.; Cueto, R.; Russo, P. S. *Langmuir* **2014**, *30*, 3373−3380.
(21) Calzolai, L.; Gilliland, D.; Garcìa, C. P.; Rossi, F. *J. Chromatogr. A* **2011**, *1218*, 4234−4239.
(22) Cho, T.; Hackley, V. *Anal. Bioanal. Chem.* **2010**, *398*, 2003−2018.
(23) Hoque, M. E.; Khosravi, K.; Newman, K.; Metcalfe, C. D. *J. Chromatogr. A* **2012**, *1233*, 109−115.

DOI: 10.1021/ac503683n
Anal. Chem. 2015, 87, 1764−1772

(24) Gray, E. P.; Bruton, T. A.; Higgins, C. P.; Halden, R. U.; Westerhoff, P.; Ranville, J. F. *J. Anal. Atom. Spectrom.* **2012**, *27*, 1532−1539.
(25) M-M, P.; Siripinyanond, A. *J. Anal. Atom. Spectrom.* **2014**, *29*, 1739−1752.
(26) Mitrano, D. M.; Barber, A.; Bednar, A.; Westerhoff, P.; Higgins, C. P.; Ranville, J. F. *J. Anal. Atom. Spectrom.* **2012**, *27*, 1131−1142.
(27) Contado, C.; Pagnoni, A. *Anal. Chem.* **2008**, *80*, 7594−7608.
(28) Hagendorfer, H.; Kaegi, R.; Traber, J.; Mertens, S. F. L.; Scherrers, R.; Ludwig, C.; Ulrich, A. *Anal. Chim. Acta* **2011**, *706*, 367−378.
(29) Giddings, J. C. *Science* **1993**, *260*, 1456−1465.
(30) Giddings, J. C.; Yang, F. J.; Myers, M. N. *Anal. Chem.* **1976**, *48*, 1126−1132.
(31) Wahlund, K. G.; Giddings, J. C. *Anal. Chem.* **1987**, *59*, 1332−1339.
(32) Litzen, A. *Anal. Chem.* **1993**, *65*, 461−470.
(33) Bendixen, N.; Losert, S.; Adlhart, C.; Lattuada, M.; Ulrich, A. *J. Chromatogr. A* **2014**, *1334*, 92−100.
(34) Du, Q.; Schimpf, M. E. *Anal. Chem.* **2002**, *74*, 2478−2485.
(35) Hartmann, R. L.; Williams, S. K. R. *J. Membr. Sci.* **2002**, *209*, 93−106.
(36) Litzen, A.; Wahlund, K. G. *J. Chromatogr. A* **1991**, *548*, 393−406.
(37) Ulrich, A.; Losert, S.; Bendixen, N.; Al-Kattan, A.; Hagendorfer, H.; Nowack, B.; Adlhart, C.; Ebert, J.; Lattuada, M.; Hungerbuhler, K. *J. Anal. Atom. Spectrom.* **2012**, *27*, 1120−1130.
(38) Gigault, J.; Hackley, V. *Anal. Bioanal. Chem.* **2013**, *405*, 6251−6258.
(39) Schachermeyer, S.; Ashby, J.; Kwon, M.; Zhong, W. *J. Chromatogr. A* **2012**, *1264*, 72−79.
(40) Kammer, F. v. d.; Legros, S.; Hofmann, T.; Larsen, E. H.; Loeschner, K. *TrAC, Trends Anal. Chem.* **2011**, *30*, 425−436.
(41) Stankus, D. P.; Lohse, S. E.; Hutchison, J. E.; Nason, J. A. *Environ. Sci. Technol.* **2010**, *45*, 3238−3244.
(42) Wahlund, K. G. *J. Chromatogr. A* **2013**, *1287*, 97−112.
(43) Kimling, J.; Maier, M.; Okenve, B.; Kotaidis, V.; Ballot, H.; Plech, A. *J. Phys. Chem. B* **2006**, *110*, 15700−15707.
(44) Lin, S. Y.; Tsai, Y. T.; Chen, C. C.; Lin, C. M.; Chen, C. h. *J. Phys. Chem. B* **2004**, *108*, 2134−2139.
(45) Westermark, G.; Kariis, H.; Persson, I.; Liedberg, B. *Colloids Surf., A* **1999**, *150*, 31−43.
(46) Yiantsios, S. G.; Karabelas, A. J. *Desalination* **1998**, *118*, 143−152.
(47) Parak, W. J.; Pellegrino, T.; Micheel, C. M.; Gerion, D.; Williams, S. C.; Alivisatos, A. P. *Nano Lett.* **2002**, *3*, 33−36.
(48) Ariza, M. J.; Benavente, J. *J. Membr. Sci.* **2001**, *190*, 119−132.
(49) Salgýn, S.; Salgýn, U.; Soyer, N. *Int. J. Electrochem. Sc.* **2013**, *8*, 4073−4084.
(50) Vrijenhoek, E. M.; Hong, S.; Elimelech, M. *J. Membr. Sci.* **2001**, *188*, 115−128.
(51) Sato, K.; Hosokawa, K.; Maeda, M. *J. Am. Chem. Soc.* **2003**, *125*, 8102−8103.

DOI: 10.1021/ac503683n
Anal. Chem. 2015, 87, 1764−1772